International Journal of
Geo-Information

MDPI

Article

Quantitative Relations between Topological Similarity Degree and Map Scale Change of Contour Clusters in Multi-Scale Map Spaces

Rong Wang [1,2], Haowen Yan [2,*] and Xiaomin Lu [2]

1 College of Resources and Environmental Engineering, Tianshui Normal University, Tianshui 741001, China; 0119061@stu.lzjtu.edu.cn
2 Faculty of Geomatics, Lanzhou Jiaotong University, Lanzhou 730070, China; xiaominlu08@mail.lzjtu.cn
* Correspondence: yanhw@mail.lzjtu.cn

Abstract: Quantitative relations between topological similarity degree and map scale change of multi-scale contour clusters are vital to the automation of map generalization. However, no method has been proposed to calculate the relations. This paper aims at filling the gap by proposing a new approach. It firstly constructed a directed contour tree by pre-processing of unclosed contours, and then developed a quantitative expression of topological relations of contour cluster based on directed contour tree. After this, it employed 108 groups of multi-scale contour clusters with different geomorphological types to explore the changing regularity of topological indices with map scale. Last, it used 416 points to calculate the quantitative relations between topological similarity degree and map scale change by curve fitting method. The results show that the quantitative expression of multi-scale topological indexes is closely related to the contour interval change, and power function is the best fit among the candidate functions.

Keywords: topological similarity degrees; map generalization; map scale change; contour clusters

check for updates

Citation: Wang, R.; Yan, H.; Lu, X. Quantitative Relations between Topological Similarity Degree and Map Scale Change of Contour Clusters in Multi-Scale Map Spaces. *ISPRS Int. J. Geo-Inf.* **2022**, *11*, 268. https://doi.org/10.3390/ijgi11040268

Academic Editors: Florian Hruby and Wolfgang Kainz

Received: 7 March 2022
Accepted: 16 April 2022
Published: 18 April 2022

1. Introduction

As one of the essential components of spatial relations, spatial similarity relation [1], including graphic similarity [2,3], topological similarity, and semantic similarity [4,5], etc., has been extensively used in human spatial cognition [6], pattern recognition [7,8], and spatial data matching [9–13]. Especially, it is an important basis of automated map generalization [14,15] guiding the generalization of maps from a larger scale (e.g., 1:5000) to a smaller scale (e.g., 1:25,000) [16].

Contour is an effective means for representing 3-dimensional topography of the real world on 2-dimensional surfaces [17], its automatic generalization is essential for downsizing small-scale topographic maps, topographic analysis based on terrain, and construction of multi-scale vector topographic map database. Indeed, map generalization is a kind of spatial similarity transformation between multi-scale maps [1]. Cartographers [18,19] believe that the key and core of contour generalization are the description of spatial relations and structure of contour. However, there is a strict order relation between contour lines, that is, spatial relation between contour lines mainly refers to topological relation [20,21]. Therefore, quantitative expression of topological relations is an important content in the study of multi-scale contour spatial similarity relations.

Generalization processes of contour include two steps: rarefaction and simplification, e.g., merge of secondary positional hilltops. When a map is generalized, if the contour intervals of the original map and the resulting map are different, some contours need to be deleted. This inevitably leads to the change of topological relations between contours. For example, there are topologically contained relations between contour line L_8 and L_5 or L_7, and topologically neighboring relation between L_5 and L_7 in the large-scale map (Figure 1a), but these topological relations no longer exist when L_5 and L_7 are merged, and L_8 is deleted in smaller scale maps. Existing research has manifested that change of topological relations and the change of map scale has a quantitative relation in map generalization [18,19]. Nevertheless, this issue has not been touched [18,19], which hampers the automation of contour cluster generalization.

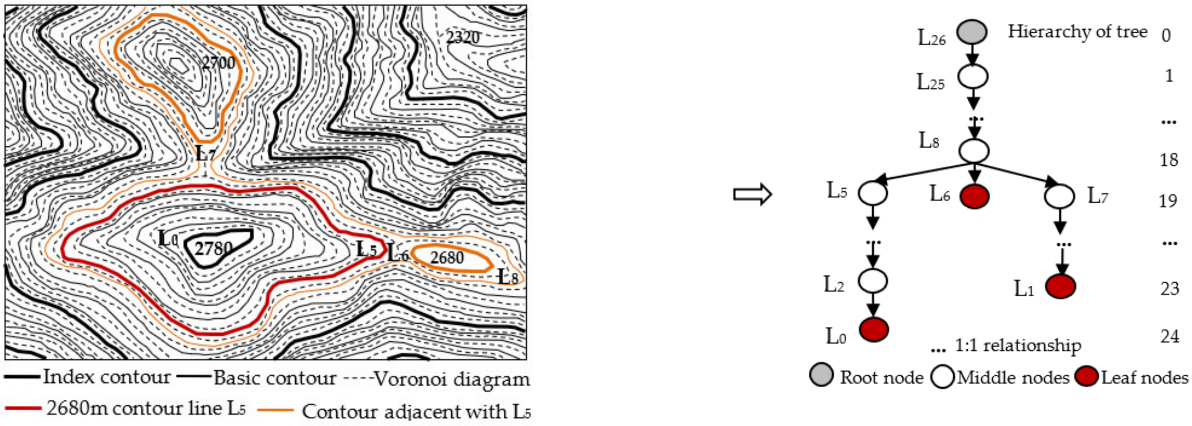

(**a**) (**b**)

Figure 1. Matching of non-closed contour (contour interval is 20 m) and its corresponding contour tree model. (**a**) Voronoi diagram and unclosed contour matching. (**b**) Directed contour tree model corresponding (**a**).

Previous studies on topological relations of contours [22–25] mainly focus on neighboring relations but do not consider topologically contained relations and topologically disjoint relations [26,27]. On the other hand, topological relations between contours are generally described using trees, but contour trees in existing achievements cannot express the topological relations reasonably. For example, in a kind of typical contour trees taking contours as nodes and the neighboring relations between contours as connecting edges [26], the relations between a parent node and its child nodes are both neighboring relations and contained relations, and in the same subtree of the contour tree, except for the topologically neighboring relations between a node and its parent node, sibling nodes, or children nodes, the relations between this node and the other nodes are all topologically disjoint. This inevitably leads to wrong calculation results of the topological relations between contours [1,27,28].

To sum up, no achievement on the quantitative relations between the change of map scale and the similarity degree between contours on maps at multiple scales has been made. Although descriptions of topological relations between contours are explored, the topological relations are not completely considered and correctly expressed using undirected contour trees [25,26]; thus, the achievements cannot be used in generalization of contour clusters such as contour extraction [29,30] and automated generalization [31–34].

The remainder of this article is structured as follows: Section 2 presents the datasets used in this study and how the datasets are pre-processed. Section 3 introduces the construction methods of directed contour trees and a quantitative expression method for topological relations of contour clusters. Section 4 demonstrates the soundness of the proposed methods using experiments. Section 5 discusses the proposed methods and the experiments shown in this study. Section 6 gives some concluding words.

2. Datasets and Their Pre-Processing

2.1. Experimental Datasets

According to different classification standards [35,36], geomorphological types can be divided into various macro-geomorphological subclasses and micro-geomorphological subtypes. To explore the quantitative relations between change of map scale and topological similarity degree of contour clusters in multi-scale map spaces, various different morphological types on multi-scale maps should be investigated. Thus, in this study 108 groups of contour clusters expressing variety of geomorphological types are selected. Each contour cluster covers 5 km × 5 km areas on the Earth surface. The source map scale of each contour cluster is 1:5000, and the target scales of corresponding generalized contours are 1:10,000, 1:50,000, 1:100,000, and 1:250,000, respectively.

Among the 108 groups of contour clusters, 104 groups are used to explore quantitative relations between change of map scale and topological similarity degree of contour clusters in multi-scale map spaces, while the other four groups, the original and target map scale are 1:5000, 1:100,000, respectively, are used to test or validate the results of quantitative relations when the contour interval change is unchanged before and after generalization. The datasets are at multiple scales (1:5000, 1:10,000, 1:50,000, 1:100,000, and 1:250,000) on the maps with different contour intervals (Table 1) and generalized manually by cartographers. They are in vector formats and provided by the National Geomatics Center of Gansu (NGCG), China.

Table 1. 104 contour clusters used in the study. (S_1, S_2, S_3, and S_4 represent the map scale of 1:10,000, 1:50,000, 1:100,000, and 1:250,000, respectively. CI and d_i represent the contour interval change and contour interval of different map scale, respectively).

Macro-Geomorphological Types (C)	Micro-Geomorphology Types (Type Encoding)	Samples	$d_i \backslash m$				CI
			S_1	S_2	S_3	S_4	
A. Loess geomorphy (5, 10, 25) 36 groups	IMiddle altitude loess tableland (A1)	Sample1–Sample15	5	20	40	100	(4, 8, 20)
	Middle and high altitude loess ridge (A2)	Sample17, Sample19–24	5	20	40	100	(4, 8, 20)
	Middle altitude loess ridge (A3)	Sample36	5	20	40	100	(4, 8, 20)
	Middle and high altitude loess ridge (A2)	Sample16, Sample18	10	20	40	100	(2, 4, 10)
		Sample25–Sample27	5	10	20	50	(2, 4, 10)
	Middle altitude loess ridge (A3)	Sample28–Sample35	5	10	20	50	(2, 4, 10)
B. Mountainous topography (5, 10, 25) 36 groups	Middle altitude and moderate relief mountain (B1)	Sample1–Sample12	10	20	40	100	(2, 4, 10)
	Middle and high altitude and moderate relief mountain (B2)	Sample18, Sample19	10	20	40	100	(2, 4, 10)
	High altitude and high relief mountain (B3)	Sample20–Sample28	10	20	40	100	(2, 4, 10)
	Middle and high altitude and high relief mountain (B4)	Sample29–Sample31	10	20	40	100	(2, 4, 10)
	Middle and high altitude and moderate relief mountain (B2)	Sample13–Sample17	5	20	40	100	(4, 8, 20)
	High altitude and moderate relief mountain (B5)	Sample32–Sample36	5	20	40	100	(4, 8, 20)
C. Fluvial landform (5, 10, 25) 32 groups	Middle altitude alluvial diluvial tableland (D1)	Sample1–Sample6	5	10	20	50	(2, 4, 10)
	Middle altitude alluvial diluvial plain (D2)	Sample12–Sample19	10	20	40	100	(2, 4, 10)
	Middle altitude diluvial plain (D3)	Sample20–Sample23	5	10	20	50	(2, 4, 10)
	Middle altitude alluvial diluvial plain (D1)	Sample7–Sample11	5	20	40	100	(4, 8, 20)
	Middle and high altitude alluvial plain (D4)	Sample24–Sample28	5	20	40	100	(4, 8, 20)
	Middle and high altitude alluvial plain (D4)	Sample29–Sample32	2.5	10	20	50	(4, 8, 20)

Table 1 shows the 104 groups of contour clusters used in the study, covering three major types of macro-geomorphological types (i.e., loess geomorphy types, mountainous types, and fluvial landforms) and various corresponding micro-geomorphological types.

2.2. Pre-Processing of the Datasets

Contours are continuous and closed in reality; however, a map is only a partial representation of the real world, and contour is stored according to sheet, which lead to contour lines are truncated into unclosed contour lines at the map border [19,37]. Secondly, contained relation is relative to closed contour lines. What is more, unclosed contour lines will lead to the uncertainty of topological relation between contour lines, which will bring unnecessary trouble to the automatic acquisition of contour elevation [38]. Thirdly, closure of unclosed contour lines will improve storage and retrieval efficiency and reduce storage space when constructing adjacency matrix and contour tree between contour lines. Therefore, in order to construct directed contour trees for the purpose of describing the topological relations between contours correctly and completely, it is necessary to preprocess the unclosed contours so that they become closed [37–39].

There are two opposite geomorphologic forms: positive topography and negative topography. Suppose contour line moves counterclockwise, if the left contour line elevations are greater than the elevation of current contour line, the geomorphologic form is positive topography, such as hills eroded by ordinary running water, mountains; otherwise, it is negative topography, such as glacial landforms, Fangshan terrain formed by horizontal rocks [28]. Taking positive topography as an example, Figure 2 shows the idea of unclosed contours closure, which consists of three steps: (i) construction of adjacency matrix based on Voronoi polygons of contours [20]; (ii) matching of unclosed contours according to the elevation field and the adjacency matrix, which includes matching of trunk contours and subtree contours; (iii) dissolving of unclosed contours according to matching field (ID_1) to closed contours, and reconstructing the binary adjacency triangular matrix ($R_{(i,j)}$) of closed contours.

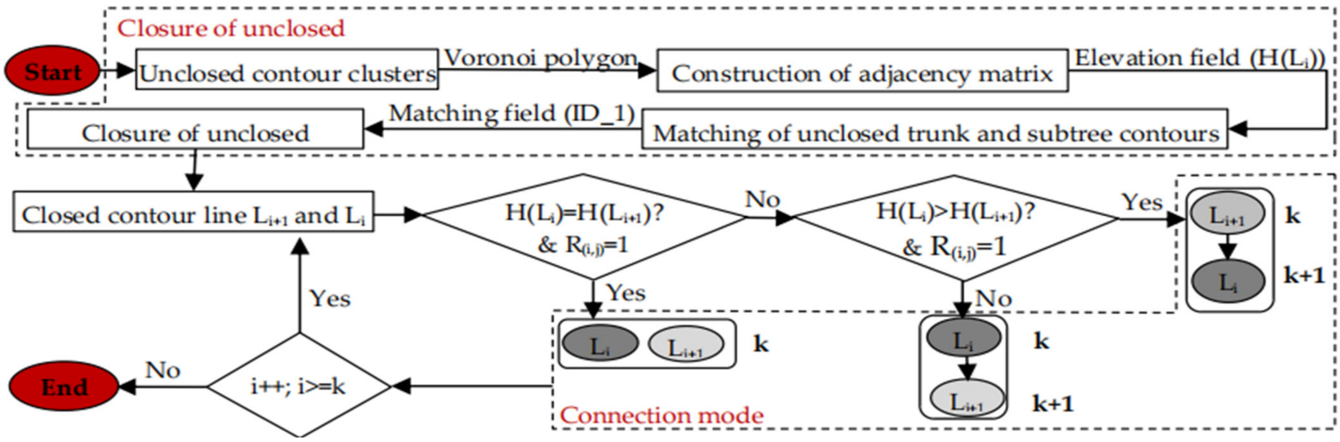

Figure 2. Closure of unclosed contours and construction of directed contour tree.

3. Methodology

3.1. Construction of Directed Contour Tree

Topological relations between contours are generally described using trees, but undirected contour tree in existing achievements cannot express the topological relations reasonably. Thus, here uses directed contour trees which can overcome the shortcomings of undirected contour trees.

The essence of constructing a directed contour tree is to determine the level (k) of contours node located in the contour tree and judge the connection mode of directed edges between nodes [19,20]. For positive topography, the elevations of the contours are arranged in equal difference and reduced from the root node corresponding to the innermost peak contours to the leaf nodes. Therefore, according to elevations and neighboring relations of closed contours, the level of contour nodes located in the directed contour tree and the connection way of the directed edges between nodes can be determined (Figure 2). Here, $k = \text{Max}\{\text{ID\_1}\} + 1 - \{\text{ID\_1}\}$, whereas, the opposite is true for negative topography. The labeled node is the root node. Repeated the same operation for the branch subtree as the trunk until all labeled nodes are traversed. If the child nodes of labeled root nodes are not unique, the child nodes need to be constantly adjusting their storage positions in the dynamic linked list to avoid crossing of directed edge. The directed contour tree of Figure 1a is showed in Figure 1b.

3.2. Quantitative Expression Method of Topological Relations

There are three types of topological relations between contours: topologically contained, topologically neighboring and topologically disjoint. Supposing that M is the total number of the nodes in a directed contour tree corresponding to the contour cluster with map scale S_1, i ($i = 1, 2, 3, \ldots, M$) is the current node. The levels of contour tree from the root node to the leaf nodes are $0, 1, 2, \ldots, k, \ldots, N$, respectively, and the total number of nodes at layer k ($k \leq N$) is P_k ($P_k \leq M$). The following paragraphs present the calculation of topologically neighboring, topological contained and topological disjoint relations.

3.2.1. Topologically Contained Relation

For the same subtree of a directed contour tree, the relations between both a node and its ancestor nodes and the node and its descendant nodes are topologically contained relations. In order to avoid repeated calculation, only the former are considered. Therefore, the total numbers of topologically contained relations of the contour cluster at scale S_1 can be expressed as:

$$T_{\text{Cont}}^{S_1} = \sum_{k=1}^{N} kP_k \tag{1}$$

Taking node L_6 in Figure 1b as an example, the relations between node L_6 and its ancestor nodes $\{L_8, \ldots, L_{25}, L_{26}\}$ are topologically contained. Thus, the contour number containing the node L_6 is equal to the level k (k = 19) that node L_6 located in the directed contour tree. Similarly, the total number of the contours containing nodes L_5 and L_7 both are 19. Thus, the total number of contours containing nodes L_5, L_6, and L_7 at 19th level of the directed contour tree is 57. Therefore, according to the total number of nodes (P_k) at each level except for the root node, the total number of topologically contained relations of the contour cluster in Figure 1a is 271.

3.2.2. Topologically Neighboring Relation

In a directed contour tree, topologically neighboring relations exist between a parent node and its child nodes or between sibling nodes, i.e., the total number of topologically neighboring relations (K_i) of node i depends on the number of its child nodes and sibling nodes, i.e., $K_i = N_i^{\text{Children}} + N_i^{\text{Siblings}}$. Thus, the total number of topologically neighboring relation of the contour cluster at scale S_1 can be calculated by:

$$T_{\text{Neigh}}^{S_1} = \sum_{i=1}^{M} K_i = \sum_{i=1}^{M} \left(N_i^{\text{Children}} + N_i^{\text{Siblings}} \right) \tag{2}$$

In order to avoid repeated calculation, topologically neighboring relations between siblings only need to be calculated once. For example, in Figure 1b, nodes L_5, L_6, and L_7 are sibling nodes to each other, L_5 is topologically neighboring with L_6, and L_6 is also topologically neighboring with L_5. In the calculation, only the former is considered. Thus, the total number of topologically neighboring relations corresponding to nodes L_5, L_6, and L_7 are 2, 1, and 0, respectively. In Figure 1b, every node has one child node except node L_8 which has three children, and each of the other nodes has no sibling nodes except nodes L_5 and L_6 have two and one, respectively. Therefore, the total number of child and sibling nodes in Figure 1b are $N_i^{\text{Children}} = 32$ and $N_i^{\text{Siblings}} = 3$, respectively. Hence, the total number of topologically neighboring relations of the contour cluster in Figure 1a is 35.

3.2.3. Topologically Disjoint Relation

The non-adjacency relations between contours except those with topologically contained and neighboring relations are called topologically disjoint relations [27]. For the same subtree of a directed contour tree, except for the topologically neighboring relations between a node and its parent node, sibling nodes, and child nodes, the relations between this node and the other nodes are all topologically disjoint. For the nodes belonging to different subtrees, except for the topologically disjoint relations between a node and its sibling nodes, the relations between a node of this subtree and the other nodes of the other subtrees are topologically disjoint, including the relations between a node of this subtree and its cousin nodes or descendant nodes of the other subtrees. Furthermore, topologically neighboring relation and topologically disjoint relation between contours complement each other in quantity. Therefore, if the number of the pairs of non-repeating nodes of the contour tree is C_M^2, the total number of topologically disjoint relations can be indirectly and quantitatively expressed by the total number of topologically neighboring relations:

$$T_{\text{Sep}}^{S_1} = C_M^2 - T_{\text{Neigh}}^{S_1} \tag{3}$$

Taking node L_7 in Figure 1b as an example, the relations between parent node L_8 and its child node L_7 is topologically contained, and the relations between node L_7 and its sibling nodes L_5 and L_6, and its child nodes are topologically neighboring. The relations between node L_7 and node L_2 and node L_0 of the other subtrees are topologically disjoint. In Figure 1b, $M = 31, C_M^2 = 465$, and the total number of topologically neighboring relations is 35. Therefore, the total number of topologically disjoint relations of the contour cluster in Figure 1a is 430.

According to the above analysis, different topological types of contour clusters intersect and complement each other in quantity. Topological relations between some nodes only need to be calculated once, e.g., topologically neighboring relations between siblings, while others need to be repetitive accumulated two times, e.g., except for the relations between parents node and children node, the topologically contained relation and topologically disjoint relation coexist between the ancestor nodes and descendant nodes in the same subtree. Therefore, how to effectively and accurately express topological relations between contours is the key and core of its quantitative expression. The total number of topological relations of the contour cluster at scale S_1 can be expressed as:

$$T_{\text{Topo}}^{S_1} = T_{\text{Cont}}^{S_1} + T_{\text{Neigh}}^{S_1} + T_{\text{Sep}}^{S_1} = \sum_{k=1}^{N} kP_k + C_M^2 \tag{4}$$

For the contour cluster in Figure 1a with the depth of directed contour tree of 25, the total number of topological relations is 736.

3.3. A Formula for Calculating Multi-Scale Topological Indexes

Analysis in Section 3.2 shows that topological indexes associated with topological quantitative expression of multi-scale contour cluster include the number ratio of multi-scale closed contours, the depth ratio of multi-scale contour tree, and multi-scale topological similarity.

3.3.1. Definition of Contour Interval Change

Contour interval is a comprehensive reflection of map scale and terrain [16]. Contour interval change can be defined as follow: supposing that there are two contour maps M_1 and M_2, M_2 is a generalized map of M_1, and their corresponding contour intervals are d_1 and d_2, respectively. The ratio d_2/d_1 is called the contour interval change (CI) from S_1 to S_2, i.e., CI = d_2/d_1.

3.3.2. Adjacent Scale Topological Index Ratio

Adjacent scale topological index ratios, including the number ratio of adjacent scale closed contours, the depth ratio of adjacent scale contour trees, and the topological total number ratio of adjacent scale contour clusters, are used to describe the change trends of topological indexes before and after generalization, which is important for human spatial cognition and understanding of change trends of multi-scale topological relations. Topological index ratio can be calculated by:

$$R_{S_1}^{S_2} = R^{S_1} / R^{S_2} \tag{5}$$

where, $R_{S_1}^{S_2}$ represents topological index ratio before and after generalization, such as depth ratio of multi-scale contour tree or number ratio of closed contours, R^{S_1} is the topological index ratio before generalization, and R^{S_2} is the topological index ratio after generalization when the contour cluster is generalized from scale S_1 to scale S_2 being $R^{S_i} = \text{Max}\{k\}+1 = N+1$ and $R_{S_1}^{S_2} \in [1, +\infty)$. Here, k is the level of the directed contour tree.

3.3.3. Multi-Scale Topological Indexes

Multi-scale topological indices, such as multi-scale topological similarity (S), multi-scale topologically contained ratio, and multi-scale topologically neighboring ratio are used to describe the quantitative variation rules of multi-scale topological relations with map scale change, which can be measured by [1]:

$$S_{S_1}^{S_2} = T_{\text{Topo}}^{S_2} / T_{\text{Topo}}^{S_1} \tag{6}$$

where, $S_{S_1}^{S_2}$ represents the multi-scale topological indices ratio of the contour cluster, which is negatively correlated with map scale change, $S_{S_1}^{S_2} \in (0,1]$; S_1 and S_2 represent the map scale of original map and the generalized map, respectively. $S_{S_1}^{S_2} \in (0,1]$. $T_{\text{Topo}}^{S_i}$ represents the total number of jth topological relations corresponding to map scale $\mathrm{S_i}$.

4. Experiments and Results

4.1. Validation of Directed Contour Trees

The reliability of constructed contour tree determines the correctness of the quantitative expression of topological relations. The elevation and code matching results of unclosed contours in Figure 1a is shown in Tables 2–4.

Table 2. Elevation and code matching of unclosed trunk contour lines.

FID	ID_1	Elev	FID	ID_1	Elev	FID	ID_1	Elev
7	0	2780	**25**	11	2580	**51**	16	2480
6	1	2760	**64**	12	2560	**52**	16	2480
11	2	2760	**65**	12	2560	**53**	17	2460
5	3	2740	**66**	12	2560	**54**	17	2460
4	4	2720	**67**	12	2560	**55**	17	2460
1	5	2700	**68**	12	2560	**56**	17	2460
3	6	2680	**39**	13	2540	**57**	17	2460
12	7	2660	**40**	13	2540	**13**	18	2440
26	8	2640	**41**	13	2540	**14**	19	2420
27	8	2640	**42**	13	2540	**37**	20	2400
28	8	2640	**43**	13	2540	**38**	20	2400
18	9	2620	**44**	14	2520	**62**	21	2380
19	9	2620	**45**	14	2520	**63**	21	2380
20	9	2620	**46**	14	2520	**58**	22	2360
29	10	2600	**47**	14	2520	**59**	22	2360
30	10	2600	**48**	14	2520	**60**	23	2340
32	10	2600	**34**	15	2500	**15**	24	2320
21	11	2580	**35**	15	2500	**16**	25	2300
22	11	2580	**36**	15	2500	**17**	26	2280
23	11	2580	**49**	16	2480			
24	11	2580	**50**	16	2480			

Table 3. Elevation and code matching of unclosed branch subtree I (FID = 11).

FID	ID_1	Elev
8	30	2680
2	29	2700
9	28	2720
10	27	2740
11	2	2760

Table 4. Elevation and code matching of unclosed branch subtree II (FID = 3).

FID	ID_1	Elev
3	6	2680

Tables 2–4 shows that the 65 unclosed contours in Figure 1a are matched and form 30 closed contours after pre-processing, including 24 trunk contours (Table 2), five branch contours of branch subtree I (Table 3), and one branch contour line of branch subtree II (Table 4). Taking Figure 1a as an example, Figure 1b indicates that the directed contour tree constructed by this method is consistent with the undirected contour tree constructed by the other existing methods [20,21], i.e., the directed contour tree construction result is more reasonable and reliable. Taking Figure 1b as an example, the total number of topologically contained relation calculated by traditional qualitative expression method based on undirected contour tree [1] is 56, and the number of fathers and sons are 27 and 29, respectively, which leads to repeated calculations the contained relations between father-son or son-father in addition to ignore the contained relations between ancestor-descendant.

4.2. Analysis of the Influencing Factors of Topological Indexes

Influence factors of topological indexes can be discovered by analyzing the distribution characteristics of the topological indexes (T_i) including average value ($\overline{X}$), standard deviation (δ), and variation coefficient (C_V). Standard deviation reflects the dispersion of a set of statistics relative to its average, and variation coefficient represents the relative fluctuation of statistical data [40]. Table 5 shows the dispersion and fluctuation of topological indices of different geomorphological types at different scales.

Some insight can be gain from Table 5.

(1) Different from topologically disjoint and topologically neighboring relation, the average of the total number of topologically contained relation of mountain topography is consistently higher than that of fluvial landform and loess geomorphy, whatever the map scale is.
(2) From different macro-geomorphological types at the same map scale perspective, the standard deviation of directed contour tree depth and the total number of topologically contained relations corresponding to mountains topography and fluvial landform is significantly greater than that of loess geomorphy. However, the variation coefficient of the total number of closed contours is just the other way around.
(3) From the viewpoint of different map scales of the same geomorphological types, with the decrease of map scale, except for variation coefficients of the total number of closed contours corresponding to mountains topography and fluvial landform remain unchanged, the standard deviation of the other topological indexes decreases gradually. In contrast, the variation coefficient of the total number of topologically disjoint relations of mountain topography gradually increases.

The above analysis manifests that both map scale and geomorphological types jointly influence the quantitative difference of topological indices, but the former is the focus of this study. Therefore, in order to realize automatic generalization of contour clusters based on multi-scale spatial similarity relations, the following contents firstly discussed the trends of multi-scale topological indexes with map scale change, and then the quantitative relations between topological similarity degree and map scale change were calculated by the curve fitting method.

Table 5. Topological indexes error statistics of different geomorphological types at different scales.

S_i	T_i	Loess Geomorphy			Mountainous Topography			Fluvial Landform		
		$\overline{X}_i$	δ	C_v	$\overline{X}_i$	δ	C_v	$\overline{X}_i$	δ	C_v
1:10,000	Depth	31.7500	13.4725	0.4243	50.2778	19.9078	0.3960	42.4848	17.4053	0.4097
	M	66.8889	31.6831	0.4737	58.2778	18.7214	0.3212	55.7273	23.1129	0.4147
	T_{Topo}	3836.0556	2819.0186	0.7349	3434.6944	2278.3595	0.6633	2544.9512	2370.9353	0.9316
	T_{Cont}	1168.2778	687.0929	0.5881	1646.3889	1123.9848	0.6827	1403.5758	1026.1380	0.7311
	T_{Sep}	2541.7222	2418.7397	0.9516	1729.6944	1144.6050	0.3254	1697.4848	1227.7492	0.7233
	T_{Neigh}	126.0556	130.8458	1.0380	58.6111	19.9007	0.6617	60.8485	25.4486	0.4182
1:50,000	Depth	9.1111	2.7545	0.3023	21.3056	10.5338	0.4944	14.6585	8.6793	0.5921
	M	18.6667	11.2122	0.6007	25.9167	11.7215	0.4523	26.0000	17.9109	0.6889
	T_{Topo}	363.4444	493.4889	1.3578	774.8056	884.0768	1.1410	719.8537	976.8114	1.3570
	T_{Cont}	137.1944	215.6154	1.5716	380.5278	441.1854	1.1594	224.5122	203.8794	0.9081
	T_{Sep}	189.5278	345.6884	1.8239	368.1111	431.0448	1.1710	424.5366	733.8932	1.7287
	T_{Neigh}	36.7222	47.2269	1.2861	26.1667	12.9692	0.4956	70.8049	173.2333	2.4466
1:100,000	Depth	4.2222	1.3117	0.3107	9.8889	5.1922	0.5251	7.3846	3.9909	0.5404
	M	7.0833	2.2216	0.3136	11.6667	5.1713	0.4433	10.0513	4.5128	0.4490
	T_{Topo}	41.8056	25.9128	0.6198	192.5833	330.3559	1.7154	93.8049	81.3432	0.8672
	T_{Cont}	17.6389	9.3202	0.5284	69.4444	67.4496	0.9713	44.0769	38.7430	0.8790
	T_{Sep}	15.7778	13.0693	0.8283	112.0000	267.8495	2.3915	43.4615	40.0025	0.9204
	T_{Neigh}	8.3889	4.6431	0.5535	11.1389	5.1556	0.4628	11.0769	7.9650	0.7191
1:250,000	Depth	1.8056	0.8218	0.4552	3.6389	2.0508	0.5657	2.7692	1.7839	0.6442
	M	3.1111	1.3044	0.4193	4.8333	2.0213	0.4182	3.7692	1.7390	0.4614
	T_{Topo}	7.2222	5.8900	0.8155	88.1944	283.1588	3.2106	13.4878	14.1512	1.0492
	T_{Cont}	3.1944	2.0677	0.6473	12.6667	12.1232	0.9571	7.6154	7.9161	1.0395
	T_{Sep}	1.3611	2.2316	1.6396	71.3611	274.7458	3.8501	3.7949	4.9746	1.3109
	T_{Neigh}	2.6667	2.2168	0.8313	4.1667	2.2104	0.5305	2.7692	1.7085	0.6170

where, Depth and M represent the depth of the contour tree and the total number of closed contours, respectively.

4.3. Quantitative Trends of Multi-Scale Topological Indexes

4.3.1. Adjacent Scale Topological Indices

Figure 3 shows the topological indexes variation trends of adjacent scale contour clusters from the same or different geomorphological type(s).

The following two conclusions can be drawn from Figure 3.

(1) Although different samples, which belong to the same map scale and micro-geomorphological types, have different contour intervals, the average of contours number ratio or the average of contour trees depth ratio is equal to the contour interval ratio of the adjacent scale contour cluster. However, due to the difference of surface relief, steep slope and surface fragmentation degree, the adjacent scale contours number ratio or the adjacent scale contour trees depth ratio is not a constant but fluctuates around the adjacent scale contour interval ratio. When the map scale change is 2.5, i.e., when contour cluster is generalized from 1:100,000 to 1:250,000, the adjacent scale topology indexes tend to be more volatile.

(2) Different from the former, the average of adjacent scale topological total number ratio is positively correlated with the corresponding contour interval ratio, but there is no proportional relation between them. For example, when the contour interval ratio of mountainous topography is {2, 2.5, 4}, the corresponding average of topological total number ratio is {5, 6, 8}. Even though the adjacent scale contour interval ratios are the same, there are significant differences in topological total number ratio for the adjacent scale contour clusters of different macro-geomorphological types, e.g., when both the former are 2.5, the latter are 15 and 8 for loess geomorphy and mountainous topography, respectively. Therefore, the following sections further explore the trends of topological similarity (i.e., the topological total number of contour cluster) with the change of map scale.

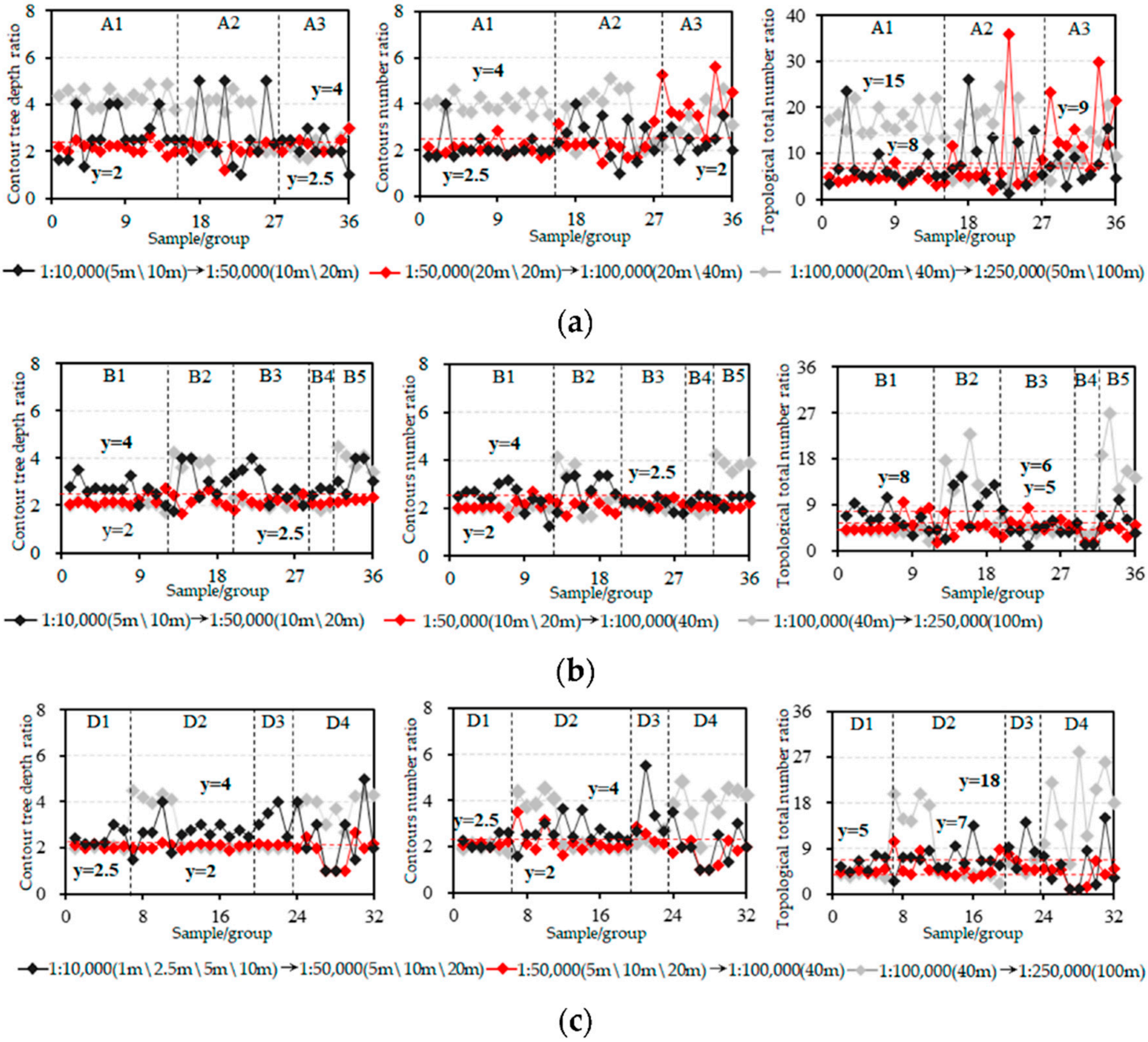

Figure 3. Topological indexes variation trends of adjacent scale contour clusters. A1–A3, B1–B3, and D1–D4 represent type codes of different micro-geomorphological types showing in Table 1. (**a**) Loess geomorphy (36 groups). (**b**) Mountainous topography (36 groups). (**c**) Fluvial landform (32 groups).

4.3.2. Multi-Scale Topological Indices

Spatial similarity degree decreases with the increase of map scale change [1]. However, the quantitative relations between multi-scale topological indexes and map scale change have not been obtained, yet. Figure 4 shows the trends of multi-scale topological similarity degree of the same or different geomorphological type(s) with map scale change, which can be described in detail by the following three points.

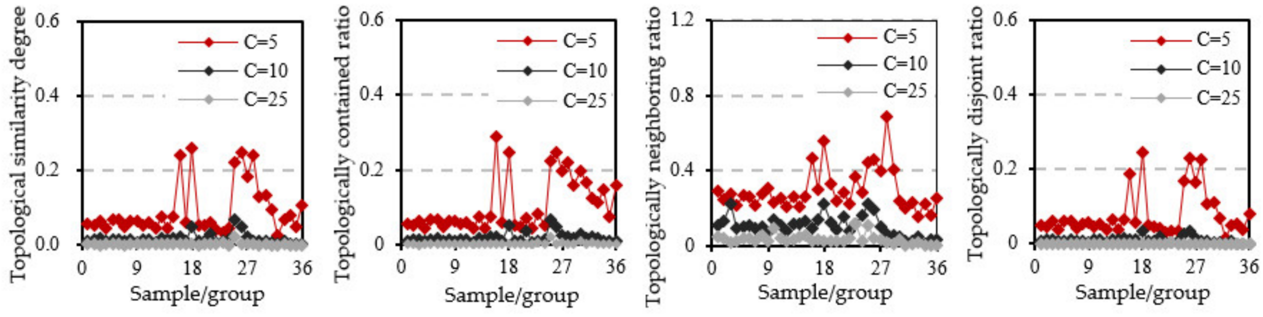

(**a**)

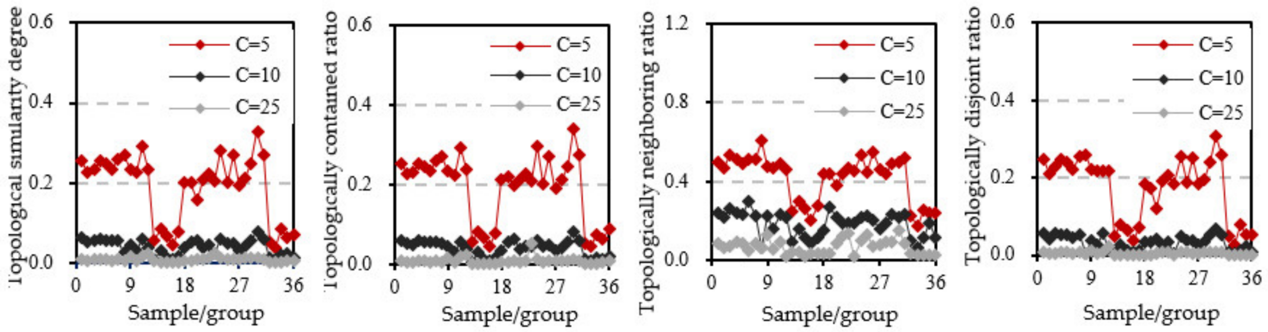

(**b**)

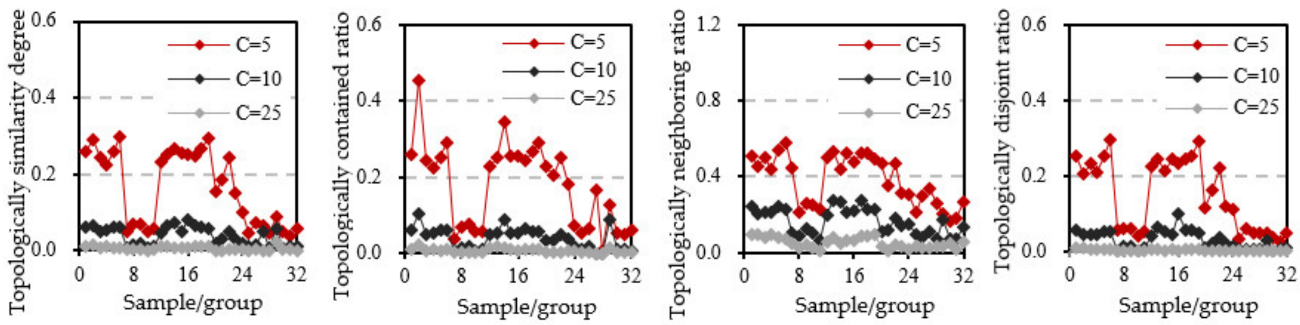

(**c**)

Figure 4. Trends of multi-scale topological similarity degree of the same or different topographic type(s) with map scale change. (**a**) Loess geomorphy (36 groups of samples). (**b**) Mountainous topography (36 groups of samples). (**c**) Fluvial landform (32 groups of samples).

(1) With the increase of map scale change, multi-scale topological index ratio decreases gradually compared within any group of samples (red line > black > gray). Nevertheless, it is not all true between different groups of samples. For example, in Figure 4b, the map scale change, contour interval change and topological similarity degrees of the 15th and 30th groups contour clusters are {10, 4, 0.0772} and {5, 4, 0.0622}, respectively. The contour interval change of the two samples is 4, and the map scale change of the former is greater than that of the latter, but topological similarity degree of the former is also larger than that of the latter.

(2) Although map scale change and macro-geomorphological type are the same, multi-scale topological index ratios of different micro-geomorphological types are remarkably different. For example, as shown by the red curve in Figure 4b, the map scale change and macro-geomorphological type of the 13th–17th groups and 1th–12th groups are the same, all belonging to mountainous topography, but micro-geomorphological type of the former is medium and high altitude and moderate relief mountains and

the latter is medium altitude and moderate relief mountains, and corresponding multi-scale topological similarity degrees fluctuate around 0.06 and 0.24, respectively. It can be known from Table 1 that the contour interval changes of the 13th–17th groups and 1st–12th groups are 4 and 2, respectively.

(3) If the contour interval changes of two groups of samples are the same, their corresponding topological indexes ratios also are very close, which all fluctuate around its average. For example, it can be known from Figure 4b and Table 1 that the contour interval change and macro-geomorphological type of the 1st–12th groups and 13th–17th groups are the same, and micro-geomorphological type of the former is medium altitude and moderate relief mountains, the latter is medium and high altitude and moderate relief mountains, micro-geomorphological type is different, but multi-scale topological similarity degrees of them are very close, which all fluctuates around 0.24.

According to above analysis, multi-scale topological indexes ratio is closely related to the contour interval change. This conclusion further indicated that "map scale change is the objective driving force of cartographic generalization [10]". Therefore, this study further formulated the quantitative relations between multi-scale topological similarity degree and map scale change of contour cluster with the same contour interval change.

4.4. Quantitative Relations between Multi-Scale Topological Similarity Degree and Map Scale Change

4.4.1. Quantitative Trends

Table 6 shows the multi-scale topological similarity degree of the same or different macro-geomorphological type(s).

(1) With the increase of map scale change, multi-scale topological similarity degree and its standard deviation decrease gradually, but variation coefficient increases gradually. For example, with the map scale change increases from 5 to 25, corresponding standard deviations of multi-scale topological similarity degree of mountainous topography decrease from 0.0849 to 0.0054, but the variation coefficients increase from 0.4501 to 0.6993, which indicated that with the increase of map scale change, the dispersion degree of multi-scale topological similarity degree decreases gradually, but the relative fluctuation between topological similarity degrees increase gradually. This trend is consistent with the results in Figure 4.

(2) If the contour interval remains unchanged before and after generalization, the multi-scale topological index ratio tends to be 1. In the experiment, four groups of multi-scale contour clusters of different micro-geomorphological types were selected and were generalized from 1:5000 to 1:10,000, and the contour interval before and after generalization is 5 m, and corresponding closed contour line number ratio, contour tree depth ratio and topological similarity degree are {0.9294, 0.9853, 0.8728}, {1, 1, 1}, {0.9881, 0.9863, 1}, and {1, 1, 0.9669}, respectively.

Considering the above analysis, the functions that conform to the trend can be listed as follows:

$$\begin{cases} S = aC^{-b}\ (a > 0, b > 0) \\ S = ae^{-bC}\ (a > 0, b > 0) \\ S = a\ln(C) + b\ \ (a > 0, b > 0) \\ S = aC + b\ \ (a < 0, b > 0) \\ S = aC^2 + bC + d\ (a > 0) \end{cases} \quad (7)$$

Table 6. Multi-scale topological similarity degrees of the same or different geomorphological type(s).

Types	C	$A1_1^1$	$A1_1^2$	$A1_1^3$	$A1_1^4$	$A1_1^5$	$A1_1^6$	$A1_1^7$	$A1_1^8$	$A1_1^9$	$A1_1^{10}$
A. Loess geomorphology	5	0.0584	0.0540	0.0664	0.0453	0.0692	0.0696	0.0498	0.0631	0.0663	0.0538
	10	0.0120	0.0144	0.0166	0.0092	0.0135	0.0162	0.0111	0.0129	0.0081	0.0158
	25	0.0035	0.0022	0.0007	0.0015	0.0027	0.0032	0.0011	0.0021	0.0016	0.0041
	C	$A1_1^{11}$	$A1_1^{12}$	$A1_1^{13}$	$A1_1^{14}$	$A1_1^{15}$	$A2_1^{16}$	$A2_1^{17}$	$A2_1^{18}$	$A2_1^{19}$	$A2_1^{20}$
	5	0.0626	0.0462	0.0756	0.0455	0.0742	0.0615	0.0545	0.0512	0.0605	0.0406
	10	0.0144	0.0077	0.0168	0.0152	0.0202	0.0122	0.0107	0.0090	0.0303	0.0073
	25	0.0029	0.0013	0.0017	0.0030	0.0040	0.0016	0.0010	0.0021	0.0023	0.0022
	C	$A2_1^{21}$	$A2_1^{22}$	$A2_1^{23}$	$A2_2^1$	$A2_2^2$	$A2_2^3$	$A2_2^4$	$A2_2^5$	$A3_2^6$	$A3_2^7$
	5	0.0327	0.0455	0.1076	0.2394	0.2603	0.2222	0.2480	0.1847	0.2406	0.1290
	10	0.0098	0.0139	0.0050	0.0207	0.0509	0.0667	0.0477	0.0213	0.0103	0.0104
	25	0.0073	0.0011	0.0011	0.0031	0.0020	0.0222	0.0032	0.0040	0.0014	0.0011
	C	$A3_2^8$	$A3_2^9$	$A3_2^{10}$	$A3_2^{11}$	$A3_2^{12}$	$A3_2^{13}$	S	δ	C_V	
	5	0.1339	0.0938	0.0244	0.0678	0.0783	0.0485	0.0924	0.0682	0.7384	
	10	0.0115	0.0062	0.0021	0.0108	0.0026	0.0041	0.0158	0.0135	0.8540	
	25	0.0041	0.0007	0.0005	0.0020	0.0003	0.0003	0.0028	0.0036	1.311	
B. Mountains geomorphy	C	$B1_2^1$	$B1_2^2$	$B1_2^3$	$B1_2^4$	$B1_2^5$	$B1_2^6$	$B1_2^7$	$B1_2^8$	$B1_2^9$	$B1_2^{10}$
	5	0.2542	0.2273	0.2344	0.2533	0.2464	0.2339	0.2599	0.2700	0.2323	0.2246
	10	0.0614	0.0530	0.0563	0.0595	0.0563	0.0565	0.0565	0.0280	0.0452	0.0301
	25	0.0088	0.0057	0.0072	0.0097	0.0087	0.0054	0.0087	0.0055	0.0148	0.0046
	C	$B1_2^{11}$	$B2_2^{12}$	$B2_2^{13}$	$B3_2^{14}$	$B3_2^{15}$	$B3_2^{16}$	$B3_2^{17}$	$B3_2^{18}$	$B3_2^{19}$	$B3_2^{20}$
	5	0.2923	0.2020	0.2018	0.1578	0.2073	0.2230	0.2025	0.2819	0.2019	0.2699
	10	0.0583	0.0376	0.0530	0.0551	0.0358	0.0441	0.0239	0.0582	0.0470	0.0474
	25	0.0149	0.0033	0.0041	0.0068	0.0091	0.0110	0.0233	0.0131	0.0097	0.0080
	C	$B3_2^{21}$	$B3_2^{22}$	$B3_2^{23}$	$B4_2^{24}$	$B4_2^{25}$	$B4_2^{26}$	$B2_1^1$	$B2_1^2$	$B2_1^3$	$B2_1^4$
	5	0.1944	0.2128	0.2318	0.2466	0.3290	0.2683	0.0561	0.0840	0.0662	0.0437
	10	0.0317	0.0426	0.0374	0.0566	0.0772	0.0589	0.0075	0.0290	0.0133	0.0091
	25	0.0084	0.0111	0.0224	0.0104	0.0110	0.0088	0.0030	0.0022	0.0009	0.0020
	C	$B2_1^5$	$B5_1^6$	$B5_1^7$	$B5_1^8$	$B5_1^9$	$B5_1^{10}$	S	δ	C_V	
	5	0.0776	0.0532	0.0371	0.0827	0.0640	0.0696	0.1887	0.0849	0.4501	
	10	0.0157	0.0123	0.0074	0.0184	0.0220	0.0136	0.0393	0.0190	0.4834	
	25	0.0018	0.0018	0.0015	0.0018	0.0036	0.0038	0.0077	0.0054	0.6993	
D. Fluvial landform	C	$D2_1^1$	$D2_1^2$	$D2_1^3$	$D2_1^4$	$D2_1^5$	$D4_1^6$	$D4_1^7$	$D4_1^8$	$D4_1^9$	$D4_1^{10}$
	5	0.0509	0.0674	0.0698	0.0507	0.0571	0.1011	0.0455	0.0722	0.0667	0.0465
	10	0.0049	0.0150	0.0181	0.0058	0.0118	0.0199	0.0094	0.0147	0.0505	0.0065
	25	0.0019	0.0020	0.0025	0.0009	0.0014	0.0027	0.0007	0.0024	0.0003	0.0003
	C	$D4_1^{11}$	$D4_1^{12}$	$D4_1^{13}$	$D4_1^{14}$	$D1_2^1$	$D1_2^2$	$D1_2^3$	$D1_2^4$	$D1_2^5$	$D1_2^6$
	5	0.0868	0.0485	0.0383	0.0559	0.2985	0.2606	0.2906	0.2449	0.2228	0.2591
	10	0.0590	0.0074	0.0096	0.0110	0.0601	0.0599	0.0656	0.0499	0.0529	0.0603
	25	0.0208	0.0013	0.0019	0.0010	0.0082	0.0110	0.0151	0.0076	0.0118	0.0077
	C	$D2_2^7$	$D2_2^8$	$D2_2^9$	$D2_2^{10}$	$D2_2^{11}$	$D2_2^{12}$	$D2_2^{13}$	$D2_2^{14}$	$D3_2^{15}$	$D3_2^{16}$
	5	0.2313	0.2523	0.2661	0.2539	0.2496	0.2491	0.2660	0.2923	0.1838	0.1548
	10	0.0472	0.0634	0.0710	0.0511	0.0789	0.0661	0.0611	0.0559	0.0283	0.0197
	25	0.0091	0.0121	0.0074	0.0084	0.0058	0.0102	0.0093	0.0098	0.0006	0.0007
	C	$D3_2^{17}$	$D3_2^{18}$	S	δ	C_V					
	5	0.2417	0.1489	0.1632	0.0973	0.5958					
	10	0.0477	0.0308	0.0379	0.0241	0.6347					
	25	0.0011	0.0012	0.0055	0.0052	0.9391					

where, A1–A3, B1–B5, and D1–D4 represent different micro-geomorphological types in Table 1. The superscript is the number of sample groups, and the subscript 1 represents the corresponding contour interval change is {4, 8, 20}, and the subscript 2 represents the corresponding contour interval change is {2, 4, 10}.

Figure 5 shows the fitting results between topological similarity degree and map scale change of multi-scale contour clusters with the same contour interval change.

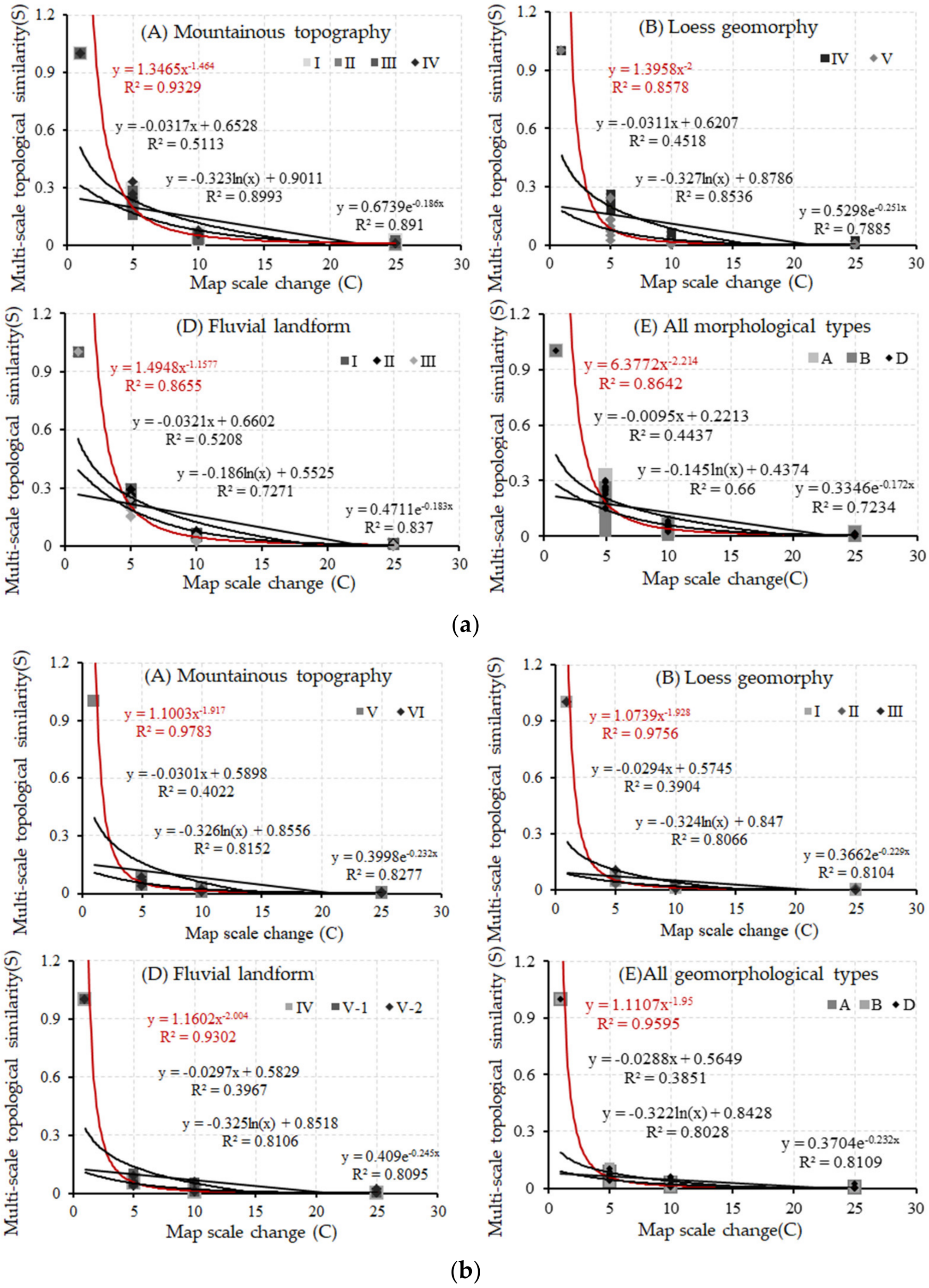

Figure 5. Fitting results between multi-scale topological similarity degree and map scale change of multi-scale contours with the same contour interval change. (**a**) Contour interval change is {1, 2, 4, 10} (57 groups of sample datasets). (**b**) Contour interval change is {1, 4, 8, 20} (47 groups of sample datasets).

Figure 5 shows that the power function (Formula (8)) is the best fit of the quantitative relations between topological similarity degree and map scale change of multi-scale contour cluster with the same contour interval change, no matter they are the same or different geomorphological type(s), the fitting precision (R^2) of power function is the highest among the candidate functions. The fitting accuracies are not less than 0.8578, and the maximum fitting accuracy is up to 0.9783. When the map scale change ranges from 1 to 5, the multi-scale topological similarity degree rapidly decreases with the increase of map scale change. Therefore, when the contour interval changes of contour clusters are the same, no matter they are the same or different geomorphological type(s), the quantitative relations between multi-scale topological similarity degree and map scale change can be expressed quantitatively using the same power function:

$$\begin{cases} S = 1\ (C = 1) \\ S = aC^{-b}\ (a > 0, b > 0) \end{cases} \tag{8}$$

4.4.2. Influence of Sample Size on the Types and Precisions of Fitting Function

It is still unknown whether the types of optimal fitting function change constantly with the increase of sample sizes. Therefore, taking the multi-scale contour cluster with the same contour interval change and different macro-geomorphological types as the research objects, Table 7 shows the influence of sample size on the type of quantitative function relations between multi-scale topological similarity and map scale change.

Table 7. Influence of sample size on the types of function fitting results.

Contour Interval Change	Sample Size (N)/Pair	Optimal Fitting Function
{1, 2, 4, 10}	N∈[4, 5], N∈N+	Exponential function
	N = 6	Power function
	N∈[7, 23], N∈N+	Exponential function
	N∈[24, 228], N∈N+	Power function
{1, 4, 8, 20}	N∈[4, 188], N∈N+	Power function

Table 7 indicates that the types of optimal fitting function constantly change with the increase of sample sizes. However, no matter which kinds of contour interval change is, power function is always the best fitting function when the sample sizes increase to a certain amount. For example, for multi-scale contour clusters, the contour interval of which is {1, 2, 4, 10}, when the sample sizes N∈[7, 23], N∈N+, the best fitting function is an exponential function, while N∈[24, 228], N∈N+, the best fitting function is power function. Plus, when the contour interval belongs to {1, 4, 8, 20}, the fitting precision (R^2) of power function is always the highest among the candidate functions, that is power function is always the best function. This conclusion further confirm that power function is the best to express the quantitative relations between multi-scale topological similarity degree and map scale change of contour cluster with the same contour interval change.

Theoretically, a complete fit R^2 = 1, but with the increase of sample size, R^2 decreases and eventually converges to a certain value. Therefore, taking contour cluster with different contour interval changes as example, Figure 6 shows the influence of sample size on the accuracy and coefficients of fitting results of power function.

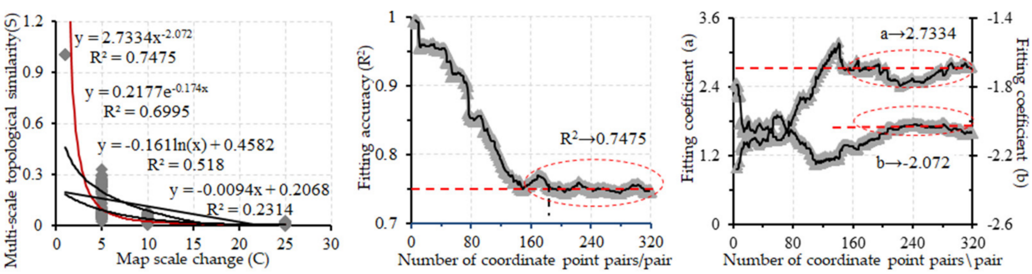

Figure 6. Fitting result of multi-scale contour cluster with the different contour interval changes.

As shown in Figure 6, power function ($S = 2.71C^{-2.07}\left(R^2 = 0.7475\right)$) also is the best to express the quantitative relations between multi-scale topological similarity degree and map scale change of contour cluster with different contour interval changes. However, the fitting accuracy is only 0.7475, and the analysis of multi-scale topological indices in Section 4.3 shows that topological indexes ratio of multi-scale contour cluster is closely related with contour interval change. Therefore, it is unreasonable to use the same power function to fit the quantitative relations between multi-scale topological similarity degree and map scale change of contour cluster with different contour interval changes.

5. Discussion

Some insights can be obtained from the above experimental results.

The quantitative expression method proposed in this paper considers and expresses topological relations using directed contour tree. Compared with traditional qualitative expression method based on undirected contour tree [1,21], directed contour tree not only sufficiently considers overlapping and complementarity between different topological types, but also effectively avoids repeated calculations and an omission of topological relations, thus it improves the accuracy of quantitative expression of topological relations. It also can be used to express topological relations of other group objects, such as intersected line networks, tree-like networks, and discrete polygon groups.

It should be noted that the multi-scale topological indices of contour clusters are closely related to the contour interval change. This can be verified from the following two aspects: firstly, when the contour intervals are unchanged before and after generalization, the average of adjacent scale contours number ratio or the average of adjacent scale contour tree depth ratio is equal to the adjacent scale contour interval ratio. In the experiment, four groups of multi-scale contour clusters of different micro-geomorphological types were selected and were generalized from 1:5000 to 1:10,000, the contour interval of both is 5 m, and the corresponding closed contour line number ratio and contour tree depth ratio are {0.9294, 1, 0.9881,1} and {0.9853, 1, 0.9863,1}, respectively. Contour lines are thinned according to a certain contour interval in the processing of generalization [21], thus this conclusion is consistent with human spatial cognition. Secondly, when map scale change and macro-geomorphological type are the same, multi-scale topological indices ratios of different micro-geomorphological types are remarkably different. However, when the contour interval changes are the same, the multi-scale topological index ratios are very close, which fluctuate around its average.

The reasons for the above trends can explained as follow: multi-scale contour topological similarity shows a consistent change law with the change of map scale change. However, different samples have different geographical characteristics, such as terrain fragmentation degree, surface relief degree, and steepness of the slope, which leads to significantly differences in topological indexes of contour cluster with the same map scale, such as Aeolian landform and dry diluvia plain, huge mountainous topography and broken hilly topography. The same is true for contour clusters with the same map scale and geomorphological type. For example, Figure 7 shows the 1:50,000 contour cluster of the same geographical type, the sparseness and slope steepness of which are significant difference. The number of closed contour lines, the depth of contour tree and the total number of topology in Figure 7b are 1.85, 2.04, and 4.07 times of Figure 7a, but one fourth, four fifth, and three fifth times of Figure 7c, respectively. The contour interval and steepness degree of slope determine the number and density of contour lines, i.e., the depth of contour tree; the fragmentation degree of terrain determines the number of nodes in each level of contour tree, these three factors together lead to significant differences in the topological indexes of contour cluster of the same scale and the same or different micro-geomorphological types.

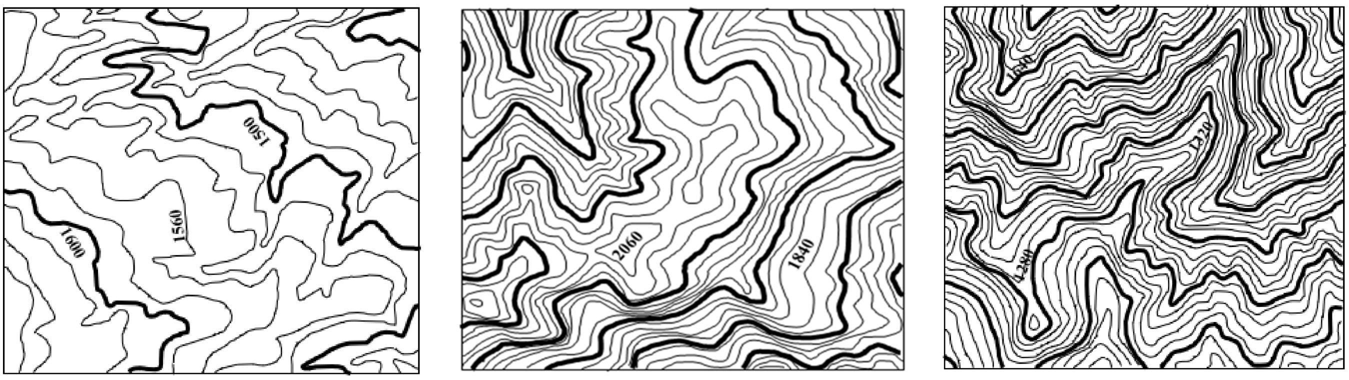

(**a**) (**b**) (**c**)

Figure 7. 1:50,000 contours with 20 m contour interval and different geographical characteristics of mountains topography. (**a**) Flat slope; (**b**) Slightly steep and slightly broken; (**c**) Steep slope.

Above experimental results can be widely used in the fields of spatial cognition, spatial reasoning, and map design. For example, if contour tree depth of the original map scale and contour interval change are known, the contour tree depth of target scale can be deduced according to the above experiment results. Topological relation between contours can be uniquely determined according to contour cluster, and vice versa, correlative position between contours can also be determined according to topological relation [38]. According to the experimental conclusion that the average of adjacent scale contour line number ratio is equal to the adjacent scale contour interval ratio, therefore, contour density should be compared according to contour interval before and after generalization in topological map design.

Furthermore, power function ($S = aC^{-b}$ ($a > 0$, $b > 0$, $C > 1$)) is the best to express the quantitative relations between multi-scale topological similarity degree and map scale change. When the numbers of the sample increase to a certain amount, the fitting accuracy, and coefficients of the power function also tend to be stable. Although the quantitative relations between multi-scale topological similarity degree and map scale change can be expressed using the same power function for multi-scale contour clusters with different contour interval changes, but the fitting accuracy is only 0.7475. Therefore, compared with multi-scale contour clusters with different contour interval changes, it is more reasonable to use the same power function to fit the quantitative relations between multi-scale topological similarity degree and map scale change of contour cluster with the same contour interval change ($R^2 \geq 0.8578$), no matter they are the same or different geomorphological type(s).

Above results are also of great significance to contour generalization. First, the establishment of contour spatial relation and the generation of contour tree provide convenient conditions and basis for the extraction of terrain structural lines [19,29]. Taking the extraction of valley line for example, the search correctness and time can be improved with the help of contour tree, when looking for the valley bottom points from the contour lines with the maximum elevation down. Second, map generalization is essentially a spatial similarity transformation between multi-scale maps, which can be measured from distance similarity, topological similarity, and direction similarity [1,27]. Therefore, multi-scale topological similarity is an important content in the research of multi-scale contour spatial similarity [19], and it is vital for the realization of contour automatic generalization. What is more, this experimental result further indicates that it is reasonable and feasible to realize the automatic generalization of contour clusters based on multi-scale spatial similarity relations.

6. Conclusions and Future Works

Obtaining topological similarity degrees among the same contour clusters on multi-scale maps is of importance in automatic map generalization. This paper developed a quantitative expression model of topological relations of contour cluster by constructing directed contour tree. On this basis, the quantitative various rules of topological indices, especially, topological similarity degrees of multi-scale contour clusters with map scale change were explored. It can be concluded that multi-scale topological indices of contour clusters are closely related to contour interval change, and power function ($S = aC^{-b}$ $(a > 0,\ b > 0)$), is the best fit to express the quantitative relations between topological similarity degree and map scale change of multi-scale contour clusters with the same contour interval change. This quantitative relation can be expressed using the same power function, no matter they are from the same or different geomorphological type(s). This conclusion indicates that it is reasonable and feasible to realize the automatic generalization of contour clusters based on multi-scale spatial similarity relations.

Currently, due to the limited contour dataset at the large scale of 1:5000 applied, only four groups of datasets, corresponding original and target map scale of which are 1:5000, 1:10,000, are used to validate the results when the map scale change is unchanged, and five kinds of map scale were considered in this study. Nevertheless, experiments indicate that the topological similarity of multi-scale contour cluster changes more acutely at small map scale change ($C \leq 5$). Therefore, in order to construct the quantitative relations between spatial similarity degree and map scale change of multi-scale contour clusters, our future study will increase the sample sizes of multi-scale dataset at large map scale, which will provide a foundation for human spatial cognition, matching of spatial data, and pattern recognition, especially, the automation of map generalization for contour clusters.

Author Contributions: All the authors contributed to the development of this manuscript. Haowen Yan and Rong Wang proposed the methodology, Rong Wang performed the experiments and wrote the draft of the manuscript; Xiaomin Lu and Haowen Yan guided the research and revised the manuscript. All authors have read and agreed to the published version of the manuscript.

Funding: This work was funded by the "National Science Foundation Committee of China (Project No.41930101; 42161066)", and Innovation Fund of Education Department of Gansu Province (No.2021A-110)".

Institutional Review Board Statement: Not applicable.

Informed Consent Statement: Not applicable.

Data Availability Statement: Multi-scale contour cluster used in this paper is provided by the National Geomatics Center of Gansu (NGCG), China. (https://www.webmap.cn/store.do?method=store&storeId=105 accessed on 6 March 2022).

Acknowledgments: This project is funded by National Science Foundation Committee of China, and the datasets is provided by NGCC. We thank them for providing funds and experimental datasets for our research. We also thank the reviewers and the editor for their insightful comments that helped us improve our manuscript.

Conflicts of Interest: The authors declare no conflict of interest.

References

1. Yan, H.W.; Li, J. *Spatial Similarity Relations in Multi-Scale Map Spaces*; Springer International Publishing: Cham, Switzerland, 2014.
2. Chehreghan, A.; Abbaspour, R.A. An assessment of spatial similarity degree between polylines on multi-scale, multi-source maps. *Geocarto Int.* **2017**, *32*, 471–487. [CrossRef]
3. Wei, Z.W.; Guo, Q.S.; Chen, L.; Liu, Y.; Tong, Y. Shape similarity measurement based on DNA alignment for buildings with multiple orthogonal features. *Acta Geod. Cartogr. Sin.* **2021**, *50*, 1683–1693.
4. Li, W.W.; Raskin, R.; Goodchil, M.F. Semantic similarity measurement based on knowledge mining: An artificial neural net approach. *Int. J. Geogr. Inf. Sci.* **2012**, *26*, 1415–1435. [CrossRef]
5. Gao, X.R.; Yan, H.W.; Lu, X.M. Semantic similarity measurement for building polygon aggregation in multi-scale map space. *Acta Geod. Cartogr. Sin.* **2022**, *51*, 95–103.
6. Li, B.; Fonseca, F. TDD: A comprehensive model for qualitative spatial similarity assessment. *Spat. Cogn. Comput.* **2006**, *6*, 31–62. [CrossRef]
7. Zhang, L.; Guilbert, E. Evaluation of river network generalization methods for preserving the drainage pattern. *Int. J. Geo-Inf.* **2016**, *5*, 230. [CrossRef]

8. Yan, X.F.; Ai, T.H.; Yang, M.; Yin, H. A graph convolution neural network for classification of building patterns using spatial vector data. *ISPRS J. Photogramm. Remote Sens.* **2019**, *150*, 259–273. [CrossRef]
9. Yan, X.F.; Ai, T.H.; Yang, M. A simplification of residential feature by the shape cognition and template matching method. *Acta Geod. Cartogr. Sin.* **2016**, *45*, 874–882.
10. Fan, H.C.; Zipf, A.; Fu, Q.; Neis, P. Quality assessment for building footprints data on OpenStreetMap. *Int. J. Geogr. Inf. Sci.* **2014**, *28*, 700–719. [CrossRef]
11. Zhao, Y.P.; Sun, Q.; Liu, X.G.; Cheng, M.; Yu, T.; Li, Y.F. Geographical entity-oriented semantic similarity measurement method and its application in road matching. *Geomat. Inf. Sci. Wuhan Univ.* **2020**, *45*, 728–735.
12. Fan, H.C.; Yang, B.S.; Zipf, A.; Rousell, A. A polygon-based approach for matching openstreetmap road network with regional transit authority data. *Int. J. Geogr. Inf. Sci.* **2016**, *30*, 748–764. [CrossRef]
13. Chehreghan, A.; Abbaspour, R.A. A geometric-based approach for road matching on multi-scale datasets using a genetic algorithm. *Cartogr. Geogr. Inf. Sci.* **2018**, *45*, 255–269. [CrossRef]
14. Ruas, A. Automating the generalization of geographical data. In Proceedings of the 20th International Cartographic Conference, Beijing, China, 18 May 2010; pp. 1943–1953.
15. Yang, W.F.; Yan, H.W.; Li, J. Formula for calculating spatial similarity degrees between point clouds on multi-scale maps taking map scale change as the only independent variable. *Geod. Geodyn.* **2015**, *6*, 113–125. [CrossRef]
16. Wang, J.Y.; He, Z.Y.; Pu, Y.X. *Cartography*; Surveying and Mapping Press: Beijing, China, 2016.
17. Li, Z.L.; Sui, H.G. An integrated technique for automated generalization of contour maps. *Cartogr. J.* **2000**, *37*, 29–37. [CrossRef]
18. Guo, R.Z. *Spatial Analysis*; Higher Education Press: Beijing, China, 2001.
19. Yan, H.W.; Wang, J.Y. *Description Approaches and Automates Generalization Algorithms for Groups of Map Objects*; The Science Press: Beijing, China, 2009.
20. Qiao, C.F.; Zhao, R.L.; Chen, J.; Chen, Y.H. A voronoi interior adjacency-based approach for generating a contour tree. *Geomat. Inf. Sci. Wuhan Univ.* **2005**, *30*, 801–804.
21. Zhang, Y.; Fan, H.; Huang, W. The method of generating contour tree based on contour Delaunay triangulation. *Acta Geod. Cartogr. Sin.* **2012**, *41*, 461–474.
22. Chen, J.; Li, C.M.; Li, Z.L.; Gold, C. A Voronoi-based 9-intersection Model for Spatial Relations. *ISPRS J. Geogr. Inf. Sci.* **2001**, *15*, 201–220. [CrossRef]
23. Chen, J.; Zhao, R.L.; Li, Z.L. Voronoi-based k-order Neighbor Relations for Spatial Analysis. *ISPRS J. Photogramm. Remote Sens.* **2004**, *59*, 60–72. [CrossRef]
24. Li, Z.L.; Huang, P.Z. Quantitative Measures for Spatial Information of Maps. *Int. J. Geogr. Inf. Sci.* **2002**, *16*, 699–709. [CrossRef]
25. Qiao, C.F.; Zhao, R.L.; Chen, J.; Chen, Y.H. A method for generating contour tree based on voronoi interior adjacency. *Geo-Spat. Inf. Sci.* **2005**, *8*, 287–290.
26. Chen, J.; Qiao, C.F.; Zhao, R.L. A Voronoi Interior Adjacency based Approach for Generating a Contour Tree. *Comput. Geosci.* **2004**, *30*, 355–367. [CrossRef]
27. Guo, W.Y.; Liu, H.Y.; Sun, Q.; Yu, A.Z.; Chen, H.X. A Contour Group Mixed Similarity Measurement Model for Region Incremental Updating. *J. Geo-Inf. Sci.* **2019**, *21*, 147–156.
28. Guo, W.Y.; Liu, H.Y.; Sun, Q.; Yu, A.Z.; Ding, Z.Y. A multisource contour matching method considering the similarity of geometric features. *Acta Geod. Cartogr. Sin.* **2019**, *48*, 643–653.
29. Ai, T.H. The drainage network extraction from contour lines for contour line generalization. *ISPRS J. Photogramm. Remote Sens.* **2007**, *62*, 93–103. [CrossRef]
30. Zhou, X.; Li, W.; Arundel, S.T. A spatio-contextual probabilistic model for extracting linear feature in hilly terrain from high-resolution DEM data. *Int. J. Geogr. Inf. Sci.* **2019**, *33*, 666–686. [CrossRef]
31. Bjorke, J.T.; Nilsen, S. Wavelets applied to simplification of digital terrain models. *Int. J. Geogr. Inf. Sci.* **2003**, *17*, 601–621. [CrossRef]
32. Ai, T.H.; Li, J.Z. A DEM generalization by minor valley branch detection and grid filling. *ISPRS J. Photogramm. Remote Sens.* **2010**, *65*, 198–207. [CrossRef]
33. Zhou, Q.M.; Chen, Y.M. Generalization of DEM for terrain analysis using a compound method. *ISPRS J. Photogramm. Remote Sens.* **2011**, *66*, 38–45. [CrossRef]
34. Chen, C.F.; Li, Y. An orthogonal least-square-based method for DEM generalization. *Int. J. Geogr. Inf. Sci.* **2013**, *27*, 154–167. [CrossRef]
35. Wang, J.Y. *Geomorphology and Its Generalization*; Surveying & Mapping Publishing House: Beijing, China, 2019.
36. Chen, W.M.; Zhou, C.H.; Li, B.Y.; Chai, H.X.; Zhao, S.M. Quantitative extraction and analysis of basic morphological types of land geomorphology in china. *J. Geogr. Sci.* **2011**, *21*, 771–790.
37. Hao, X.Y. *Map Information Recognition and Extraction Technology*; Surveying & Mapping Publishing House: Beijing, China, 2001.
38. Wu, H.H. *GIS and Basic Model and Algorithm of Map Information Generalization*; Wuhan University Press: Wuhan, China, 2012.
39. Guo, Q.S.; Wu, H.H.; Li, P.C. Spatial relation rules and progressive graphic simplification of contours. *Geomat. Inf. Sci. Wuhan Univ.* **2000**, *25*, 31–34.
40. Nigel, W. *Geographical Data Analysis*; Wiley & Sons Ltd.: New York, NY, USA, 1995.